REFERENCES AND NOTES

1. R. J. Cabelli, A. Hohn, C. J. Shatz, *Science* **267**, 1662 (1995); S. Cohen-Cory and S. E. Fraser, *Nature* **378**, 192 (1995); P. Caroni and M. Becker, *J. Neurosci.* **12**, 3849 (1992); P. Caroni and P. Grandes, *J. Cell Biol.* **110**, 1307 (1990).
2. C. G. Causing *et al.*, *Neuron* **18**, 257 (1997).
3. W. D. Snider and J. W. Lichtman, *Mol. Cell. Neurosci.* **7**, 433 (1996).
4. C. E. Henderson *et al.*, *Science* **266**, 1062 (1994).
5. L. J. Houenou, R. W. Oppenheim, L. X. Li, A. C. Lo, D. Prevette, *Cell Tissue Res.* **286**, 219 (1996).
6. Q. Yan, C. Matheson, O. T. Lopez, *Nature* **373**, 341 (1995).
7. D. E. Wright and W. D. Snider, *Cell Tissue Res.* **286**, 209 (1996).
8. M. Yamamoto, G. Sobue, K. Yamamoto, S. Terao, T. Mitsuma, *Neurochem. Res.* **21**, 929 (1996).
9. A mouse GDNF cDNA was cloned by the reverse transcription polymerase chain reaction (RT-PCR) using total RNA from embryonic (E13) head as template. A 700-bp Bam HI fragment, containing the full-length cDNA for mouse GDNF, was cloned into the plasmid cassette pMyo-hGH, containing a 1.6-kb Hind III–Kpn I fragment, corresponding to myogenin promoter (*10*–*11*), and a 2.1-kb Bam HI–Hind III fragment, containing human growth hormone gene including a polyadenylation signal. The resulting plasmid pMyo-GDNF was digested with Not I and Xho I; the 4.4-kb transgene fragment was eluted from an agarose gel and used for pronuclear injection (B6/CBA strain). Integration of the transgene into the mouse genome was determined by PCR on genomic DNA from mouse tail using the 5′-oligo (5′-TGATGTGGTAGTGGTAGGTCT-3′) and the 3′-oligo (5′-CAGGCATATTGGAGTCACTGG-3′). Genotype was confirmed by Southern (DNA) blot analysis as described (*11*) using a 0.7-kb digoxigenin-labeled PCR product, corresponding to the mouse GDNF cDNA as a probe.
10. T. C. Cheng, T. A. Hanley, J. P. Mudd, *J. Cell Biol.* **119**, 1649 (1992); J. P. Merlie, J. Mudd, T. C. Cheng, E. N. Olson, *J. Biol. Chem.* **269**, 2461 (1994).
11. D. E. Wright, L. Zhou, J. Kucera, W. D. Snider, *Neuron* **19**, 503 (1997).
12. The amount of GDNF mRNA in the muscle of F_1 offspring from different transgenic lines was assessed by in situ hybridization on cryostat sections (16 μm) of P1 mice cut in the transverse plane at the level of the forelimbs using riboprobes to GDNF, as described (*7*).
13. Amounts of GDNF protein in muscle homogenate were measured using the GDNF E_{max} immunoassay kit (Promega), following the manufacturer's instructions using whole muscles (upper hind limbs) dissected from P3 and adult animals.
14. Q. T. Nguyen and J. W. Lichtman, *Curr. Opin. Neurobiol.* **6**, 104 (1996).
15. Mice were anesthetized and a ventral midline incision was made to expose sternomastoid muscles. Tetramethyl rhodamine isothiocyanate α-bungarotoxin (TRITC-αBTX, 5 μg/ml; Molecular Probes) was applied to the muscles (20 min) to label postsynaptic acetylcholine receptors (AChRs). After transcardial perfusion with 2% paraformaldehyde, whole sternomastoid muscles were dissected and pinned on a Sylgard-lined dish. Nerve terminals and axons were labeled with antibodies to neurofilament (SMI312, Sternberger) and synaptic vesicles (G95, P. Greengard). NMJs doubly labeled for nerve terminals and AChRs were viewed with high-numerical-aperture objectives with confocal optics using a real-time scanner (Noran, Odyssey). The number of incoming axons could be accurately defined by carefully focusing through the region of the NMJ where the nerves enter.
16. T. Tsuzuki *et al.*, *Oncogene* **10**, 191(1995); D. C. Molliver *et al.*, *Neuron* **19**, 849 (1997).
17. Whole diaphragm muscles with an intact portion of the phrenic nerve were dissected from P9–P10 mice in oxygenated culture medium (Dulbecco's). Electrophysiological recordings of numbers of axons innervating single muscle fibers were made using intracellular recording as described [P. A. Redfern, *J. Physiol. (London)* **209**, 701 (1970)] in the presence of 1 to 3 μM curare to prevent muscle contraction.
18. P6–P8 mice were anesthetized and a ventral midline incision was made to expose the left sternomastoid muscle. Motor neurons that innervate the sternomastoid muscle were retrogradely labeled with Fluoro-Gold (Fluorochrome) as described [D. M. Rotto-Percelay *et al.*, *Brain Res.* **574**, 291 (1992)]. Briefly, three separate injections (200 to 400 nl) of 4% Fluoro-Gold in saline were made into the left sternomastoid muscle. The wound was sutured closed and the mouse pups were returned to their mother. At P11 (3 to 5 days later), the pups were reanesthetized; brainstem and spinal cords were processed for motor neuronal cell counting with the following changes: Brainstem and spinal cords were cut in the horizontal plane at 12 μm, mounted serially on glass slides, counterstained with ethidium bromide [L. C. Schmued, L. W. Swanson, P. E. Sawchenko, *J. Histochem. Cytochem.* **30**, 123 (1982)], and coverslipped in glycerin. Fluoro-Gold–labeled neurons were examined with a fluorescence microscope with an ultraviolet filter set (Leica) and imaged with a silicon-intensified camera. As a precaution to prevent errors associated with double counting, only cells in which a nucleus could be seen were counted and adjacent sections were compared [physical dissector; R. E. Coggeshall, *Trends Neurosci.* **15**, 9 (1992)].
19. P9–P10 mice were perfused transcardially with 2% paraformaldehyde. The nerve to the sternomastoid muscle was dissected and stored in a 2% paraformaldehyde–2% glutaraldehyde solution for 5 to 6 hours. After an overnight rinse in 5% sucrose in phosphate-buffered saline, nerves were stained in 1% osmium tetroxide. Plastic sections (1 μm) were serially mounted and stained with 1% toluidine blue–1% sodium borate. Cross sections of the nerve were photographed under a dissecting scope (50×) and the number of myelinated axons (of all diameters) counted.
20. Whole sternomastoid muscles with an intact portion of the incoming nerve were dissected from P10 mice in oxygenated culture medium (Dulbecco's). Motor unit twitch tension recordings using a force transducer (Cambridge Neuroscience) were performed as described [W. J. Betz, J. H. Calwell, R. R. Ribchester, *J. Physiol. (London)* **297**, 463 (1979)].
21. M. R. Pranzatelli, *Clin. Neuropharmacol.* **13**, 329 (1990).
22. N. P. Rosman, J. H. Donelly, M. A. Braun, *J. Dev. Behav. Pediatr.* **54**, 263 (1984).
23. M. C. Brown, J. K. Jansen, D. Van Essen, *J. Physiol. (London)* **261**, 387 (1976); T. Fladby, *Acta Physiol. Scand.* **129**, 229 (1987).
24. Q. T. Nguyen, J. W. Lichtman, A. Sh. Parsadanian, W. D. Snider, data not shown.
25. R. W. Oppenheim, *Neuron* **17**, 195 (1996).
26. Q. Yan *et al.*, *J. Neurobiol.* **24**, 1555 (1993).
27. C. E. Henderson *et al.*, *Nature* **363**, 266 (1993).
28. V. E. Koliatsos *et al.*, *Proc. Natl. Acad. Sci. U.S.A.* **91**, 3304 (1994).
29. H. Funakoshi *et al.*, *Science* **268**, 1495 (1995).
30. M. Brenner, W. C. Kisseberth, Y. Su, F. Besnard, A. Messing, *J. Neurosci.* **14**, 1030 (1994).
31. C. R. Keller-Peck, A. Sh. Parsadanian, L. Zhou, W. D. Snider, *Soc. Neurosci. Abstr.* **23**, 620 (1997).
32. Y. W. Kwon, S. J. Abbondanzo, C. L. Stewart, M. E. Gurney, *J. Neurobiol.* **28**, 35 (1995); C. L. Jordan, *Dev. Neurosci.* **18**, 185 (1996); A. W. English and G. Schwartz, *Dev. Biol.* **169**, 57 (1995).
33. B. Blondet *et al.*, *Dev. Biol.* **132**, 153 (1989).

34. We thank L. Worley for excellent technical assistance. Supported by grants from NIH and the Muscular Dystrophy Association.

23 October 1997; accepted 21 January 1998

Conservation of T Cell Receptor Conformation in Epidermal γδ Cells with Disrupted Primary V_γ Gene Usage

Caroline A. Mallick-Wood, Julia M. Lewis, Lauren I. Richie, Michael J. Owen, Robert E. Tigelaar,* Adrian C. Hayday*†

A feature that distinguishes γδ T cell subsets from most αβ T cells and B cells is the association of expression of single T cell receptor (TCR) γ and δ variable (V) region gene segments with specific anatomic sites. Mice lacking the TCR $V_\gamma5$ chain normally expressed by most dendritic epidermal T cells were shown to retain a conformational determinant (idiotype) ordinarily expressed exclusively by such $V_\gamma5^+$ cells. Conservation by shuffled γδ TCR chains of an idiotype associated with a specific anatomic site indicates that for TCRγδ, as for immunoglobulin, conformation is associated to a greater extent with the function or development of lymphocyte repertoires than is the use of particular gene segments.

The efficacy of the adaptive immune system depends on its capacity to recognize pathogens in a highly antigen-specific manner. B cells and αβ T cells recognize antigens through surface immunoglobulin (Ig) and TCRs, respectively. Although γδ cells regulate immune responses to protozoal, bacterial, and viral infection (*1*, *2*), neither their primary physiological functions nor their antigen specificities have been fully clarified.

A characteristic feature of γδ cells is the association of single γ and δ chains with γδ cell subsets in specific anatomic sites. For example, most human peripheral blood γδ cells express $V_\gamma9$ and $V_\delta2$ chains of relatively limited diversity (*3*). More extreme examples occur in murine epithelia. Essentially all reproductive tract γδ cells express a canonical $V_\gamma6$-$V_\delta1$ TCR, whereas 60 to >99% of dendritic epidermal T cells (DETCs)—variation depending on strain and age of the mice—express a canonical $V_\gamma5$-$V_\delta1$ TCR (*4*), which can be detected with the monoclonal antibody (mAb) 17D1 (*5*). Ordinarily, 17D1 does not react

with any other γδ cells, including those of the reproductive epithelium that share with DETCs use of the identical $V_\delta1$ chain. Such site-specific homogeneity of antigen receptor expression had not been observed in previous studies of αβ T cells and B cells. To investigate this feature of γδ cells, we examined the effect on DETC development of $V_\gamma5$ gene disruption (6) (Fig. 1).

To confirm $V_\gamma5$ gene disruption, we stained epidermal sheets (7) from $V_\gamma5^{-/-}$ and $V_\gamma5^{+/+}$ littermates with mAbs to $V_\gamma5$, TCRδ, and CD3ε (Fig. 2). $V_\gamma5^+$ cells were readily detectable in epidermis from $V_\gamma5^{+/+}$ mice, but not in that from $V_\gamma5^{-/-}$ mice. Nonetheless, dendritic $CD3^+TCR\delta^+$ DETCs were present in $V_\gamma5^{-/-}$ mice at densities not significantly different from those in $V_\gamma5^{+/+}$ controls (153 ± 26 versus 221 ± 79/mm^2, respectively; $P = 0.54$).

Because normal DETCs do not readily develop in mice lacking either TCRδ (8) or p72 SYK, a putative transducer of signals from the DETC TCR (9), the development of a DETC repertoire in $V_\gamma5^{-/-}$ mice implied that other γδ TCRs could substitute for $V_\gamma5$-$V_\delta1$. To determine whether those TCRs were similar in structure to the canonical DETC TCR, we examined the "replacement" repertoire with mAb 17D1. This mAb was generated by immunizing Lou/M rats with a DETC line, fusing splenocytes with the SP2/0 myeloma, and screening the resulting mAbs for reactivity with DETCs but not with peripheral T or natural killer cells. From a DETC clone (1D2), both 17D1 and a pan antibody to TCRδ (3A10) immunoprecipitated proteins (*10*) of sizes similar to those previously described for the 1D2 γδ TCR (*11*) (Fig. 3A). Moreover, pretreatment of lysates with 3A10 removed all 17D1 immunoreactivity, whereas pretreatment with 17D1 removed all 3A10 immunoreactivity (Fig. 3A). These results placed the 17D1 epitope on the TCR. However, 17D1 yielded negligible staining with either reproductive tract γδ cells or five hybridomas that express the same $V_\delta1$-$D_\delta2$-$J_\delta2$ chain as DETCs (*12*), but paired with $V_\gamma6$ rather than with $V_\gamma5$ (Table 1). Thus, 17D1 reactivity could not be attributed simply to the expression of $V_\delta1$-$D_\delta2$-$J_\delta2$. Indeed, among 19 hybridomas and cell lines expressing different TCR γδ chain combinations (Table 1), 17D1 reacted only with those expressing both $V_\delta1$ and $V_\gamma5$, consistent with it defining a characteristic DETC TCR conformation.

Unexpectedly, however, the same conformation was detected in epidermal sheets from $V_\gamma5^{-/-}$ mice (Fig. 2). Flow cytometry of epidermal cells (*13*) from individual mice showed that 33 ± 13% ($n = 6$) of the $TCR\gamma\delta^+$ DETCs from $V_\gamma5^{-/-}$ mice were $17D1^+$, compared with a value of 78 ± 18%

C. A. Mallick-Wood, L. I. Richie, A. C. Hayday, Department of Molecular, Cell, and Developmental Biology and Section of Immunobiology, Yale University, New Haven, CT 06520, USA.
J. M. Lewis and R. E. Tigelaar, Department of Dermatology and Section of Immunobiology, Yale University, New Haven, CT 06511, USA.
M. J. Owen, Imperial Cancer Research Fund, Lincoln's Inn Fields, London WC2A 3PX, UK.
*These authors contributed equally to this report.
†To whom correspondence should be addressed. E-mail: adrian.hayday@yale.edu

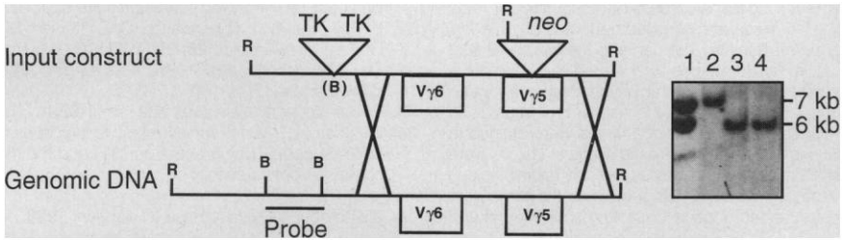

Fig. 1. Disruption of the $V_\gamma5$ gene. A 7-kb Balb/c genomic clone that contains both $V_\gamma5$ and $V_\gamma6$ coding regions was used to generate the $V_\gamma5$ disruption construct. The $V_\gamma5$ gene was disrupted by insertion of a neomycin resistance gene (*neo*) under the control of a phosphoglycerate kinase gene promoter into an Eco RV site in the $V_\gamma5$ coding region. A 3-kb Bgl II fragment was deleted to generate a unique Bgl II site [(B)], into which two herpes simplex virus thymidine kinase genes (*TK*) were inserted. The 3-kb Bgl II fragment was subsequently used as a probe in Southern blot analysis, detecting a 7-kb Eco RI (R) genomic fragment in the germline configuration and a 6-kb Eco RI fragment from the recombinant allele. Lane 1, Eco RI–digested DNA from targeted 129 embryonic stem cell clone 21.2; lanes 2 to 4, Eco RI–digested tail DNA of $V_\gamma5^{+/+}$, $V_\gamma5^{-/-}$ male, and $V_\gamma5^{-/-}$ female mice, respectively.

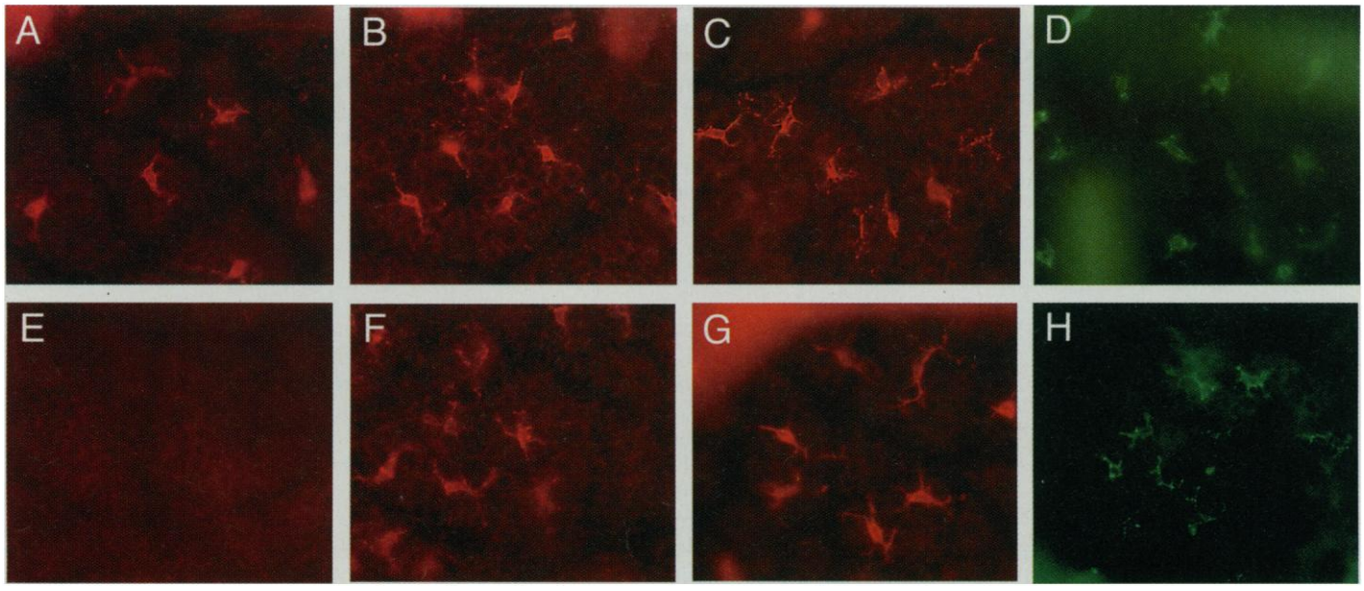

Fig. 2. Epidermal sheets prepared from $V_\gamma5^{+/+}$ (**A** to **D**) and $V_\gamma5^{-/-}$ (**E** to **H**) mice and stained with antibodies to $V_\gamma5$ (A and E), antibodies to CD3 (B and F), antibodies to TCRδ (C and G), or mAb 17D1 (D and H) (*7*). Original magnification, ×400. Data are representative of 10 fields of 0.042 mm^2 per specimen, two to six specimens per mouse, two mice per experiment, and three experiments.

($n = 5$) for $V_\gamma5^{+/+}$ littermates. To investigate the basis for 17D1 epitope expression on $V_\gamma5^{-/-}$ DETCs, we applied reverse transcription polymerase chain reaction (RT-PCR) analysis (*14*) to a $17D1^+$ DETC clone (30B4) derived from $V_\gamma5^{-/-}$ DETC mice (*15*). Transcripts of $V_\gamma1$-$J_\gamma4$ and $V_\delta1$-$J_\delta2$, but not of $V_\gamma4$, -5, -6, or -7 or $V_\delta4$ or $V_\delta6$, were detected (*16*). Sequencing revealed a simple, in-frame $V_\gamma1$-$J_\gamma4$ join, identical to that of the thymic hybridoma AA37 (*17*). The join, devoid of non–template-encoded nucleotides, might have been generated by recombination mediated by small stretches of sequence homology, which is common in fetal thymic V(D)J recombination (*8*, *18*). Sequencing of the $V_\delta1$-$J_\delta2$ product likewise revealed a simple, in-frame join, identical to the canonical $V_\delta1$-$D_\delta2$-$J_\delta2$ junctions present in day-13 to day-17 fetal thymocytes, in DETCs, in reproductive tract γδ cells, and in a subset of the cell lines and hybridomas listed in Table 1 (*4*, *12*).

Independent evidence for the association of this $V_\gamma1$-$V_\delta1$ chain pairing with the 17D1 epitope was provided by PCR and restriction fragment length polymorphism (RFLP) analysis (*19*) of polyclonal $17D1^+$ DETCs that were sorted by flow cytometry from a different $V_\gamma5^{-/-}$ mouse. The analysis detected the canonical $V_\delta1$-$J_\delta2$ rearrangement and only a single $V_\gamma1$-$J_\gamma4$ rearrangement, which was of the size predicted for the in-frame 30B4 join. Moreover, the predominant sequence obtained from the polyclonal population was identical to that of 30B4, with the exception of a conservative (serine to threonine) switch at the V-J junction (*16*).

Flow cytometry confirmed that clone 30B4 expressed $V_\gamma1$ (Fig. 3B), as did other $V_\gamma5^-$, $17D1^+$ cells. $V_\gamma1$ expression has been previously detected in the epidermis of normal mice and in hybridomas derived therefrom (*20*), but not in combination with either $V_\delta1$ or the 17D1 epitope. Several $17D1^-$ lines and clones that were likewise isolated from $V_\gamma5^{-/-}$ epidermis expressed various TCRs, including $V_\gamma7$ (Fig. 3B), $V_\gamma4$, and $V_\gamma1$. $V_\gamma7$ is often present in the gut paired with $V_\delta4$ (*21*, *22*), but has not previously been identified in the epidermis. No $V_\gamma7^+$ DETC clones stained with antibodies to $V_\delta4$, although a $V_\delta4^+V_\gamma7^-$ DETC line was isolated. Thus, DETCs in $V_\gamma5^{-/-}$ mice constitute a distinct repertoire, including $V_\gamma1^+$ cells that retain the 17D1-defined TCR conformation, ordinarily characteristic of $V_\gamma5$-$V_\delta1$ DETCs.

Conventional $V_\gamma5$-$V_\delta1$ DETCs secrete interleukin-2 (IL-2) in response to PAM2.12 transformed keratinocytes (*23*). This TCR-dependent activity was also exhibited by the $17D1^+$ clone 30B4, and by

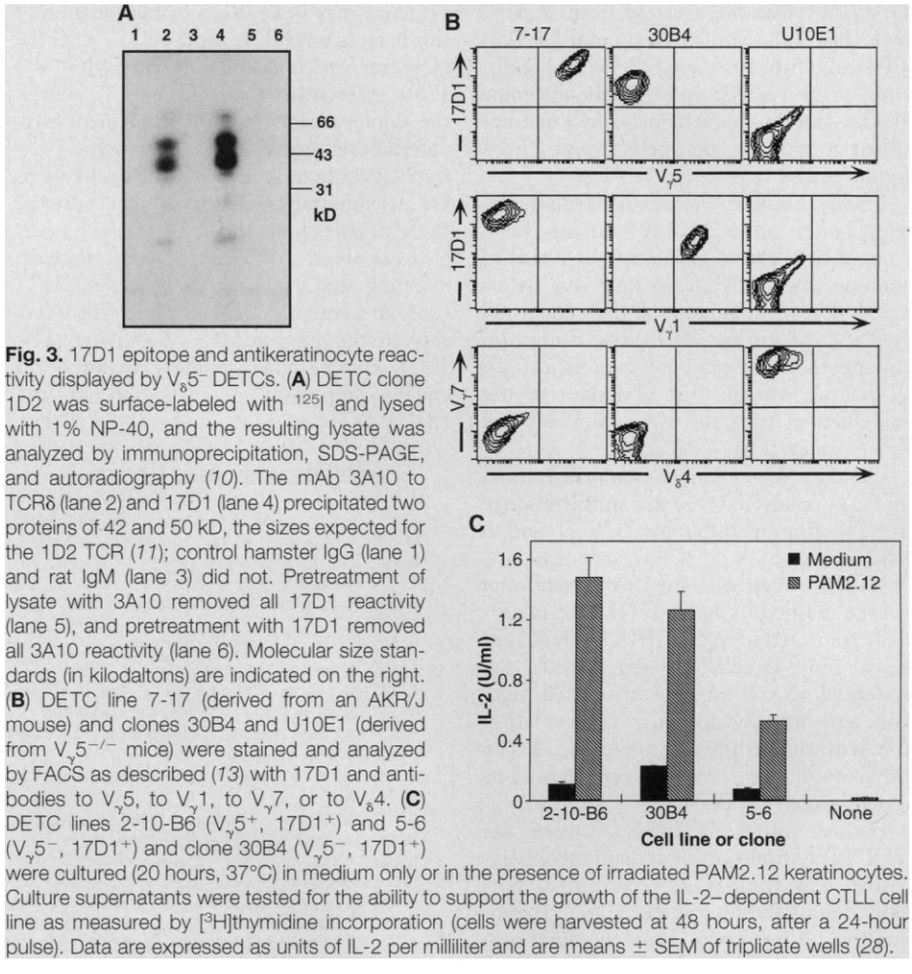

Fig. 3. 17D1 epitope and antikeratinocyte reactivity displayed by $V_\delta5^-$ DETCs. (**A**) DETC clone 1D2 was surface-labeled with ^{125}I and lysed with 1% NP-40, and the resulting lysate was analyzed by immunoprecipitation, SDS-PAGE, and autoradiography (*10*). The mAb 3A10 to TCRδ (lane 2) and 17D1 (lane 4) precipitated two proteins of 42 and 50 kD, the sizes expected for the 1D2 TCR (*11*); control hamster IgG (lane 1) and rat IgM (lane 3) did not. Pretreatment of lysate with 3A10 removed all 17D1 reactivity (lane 5), and pretreatment with 17D1 removed all 3A10 reactivity (lane 6). Molecular size standards (in kilodaltons) are indicated on the right. (**B**) DETC line 7-17 (derived from an AKR/J mouse) and clones 30B4 and U10E1 (derived from $V_\gamma5^{-/-}$ mice) were stained and analyzed by FACS as described (*13*) with 17D1 and antibodies to $V_\gamma5$, to $V_\gamma1$, to $V_\gamma7$, or to $V_\delta4$. (**C**) DETC lines 2-10-B6 ($V_\gamma5^+$, $17D1^+$) and 5-6 ($V_\gamma5^-$, $17D1^+$) and clone 30B4 ($V_\gamma5^-$, $17D1^+$) were cultured (20 hours, 37°C) in medium only or in the presence of irradiated PAM2.12 keratinocytes. Culture supernatants were tested for the ability to support the growth of the IL-2–dependent CTLL cell line as measured by [^{3}H]thymidine incorporation (cells were harvested at 48 hours, after a 24-hour pulse). Data are expressed as units of IL-2 per milliliter and are means ± SEM of triplicate wells (*28*).

Table 1. Analysis of cell lines and hybridomas of known TCR composition by flow cytometry (*13*) for reactivity with mAb 17D1 and mAbs to TCRγδ (3A10 or GL3).

Hybridoma or cell line	TCR composition	Reactivity	
		17D1	TCRγδ mAb
BW5147*		–	–
153*	$V_\gamma5$-$V_\delta1$	+	+
1D2†‡	$V_\gamma5$-$V_\delta1$	+	+
119*‡	$V_\gamma5$-$V_\delta1$	+	+
V17*	$V_\gamma5$-$V_\delta2$	–	+
66*‡	$V_\gamma6$-$V_\delta1$	–	+
21*‡	$V_\gamma6$-$V_\delta1$	–	+
90BPL1‡§	$V_\gamma6$-$V_\delta1$	–	+
90BPL2‡§	$V_\gamma6$-$V_\delta1$	–	+
90BPL3‡§	$V_\gamma6$-$V_\delta1$	–	+
33BTE1409§	$V_\gamma6$-$V_\delta1$	–	+
1*	$V_\gamma4$-$V_\delta7$	–	+
KN6*	$V_\gamma4$-$V_\delta5$	–	+
KN102*	$V_\gamma4$-$V_\delta5$	–	+
KN106*	$V_\gamma7$-$V_\delta5$	–	+
T195‖	$V_\gamma1$-$V_\delta6.2$	–	+
AA37‖	$V_\gamma1$-$V_\delta6.2$	–	+
BB27‖	$V_\gamma1$-$V_\delta6.2$ and $V_\gamma4$	–	+
Y245‖	$V_\gamma1$-$V_\delta Z49$ and $V_\gamma4$	–	+
Y93A.1‖	$V_\gamma1$-$V_\delta6.1$ and $V_\gamma4$	–	+

*Fetal thymocyte hybridomas (*12*, *29*) were analyzed by M. Bonneville. †DETC clone 1D2 was produced by Takashima *et al.* (*30*). ‡Seven cell lines and hybridomas with the same $V_\delta1$-$D_\delta2$-$J_\delta2$ canonical join (*12*, *29*, *31*). §Hybridomas provided by W. Born (*31*). ‖DETCs expressing noncanonical TCRs as well as the thymocyte hybridomas AA37 and BB27 were provided by E. Shevach.

the 17D1$^+$ line 5-6 isolated from $V_\gamma5^{-/-}$ mice (Fig. 3C). Similar to normal DETCs, 30B4 and 5-6 also lysed PAM2.12 cells. Thus, 17D1$^+$ cells from $V_\gamma5$-deficient mice could respond to keratinocytes in a manner similar to that of such cells derived from normal mice.

Finally, because $V_\gamma5^+$ cells normally develop before other TCR$\gamma\delta^+$ subsets (*24*), we used flow cytometry and PCR-RFLP to examine whether $V_\gamma5$ mutation overtly affected the development of the remaining TCR$\gamma\delta^+$ repertoire. No gross disruption was apparent. For example, canonical $V_\gamma6$-$J_\gamma1$ rearrangements were abundant in the reproductive tract of both $V_\gamma5^{+/+}$ and $V_\gamma5^{-/-}$ mice (*16*).

Our data show that an outwardly normal DETC population developed in the absence of $V_\gamma5$. Among different TCR γ and δ pairings used by $V_\gamma5^-$ DETCs, at least one ($V_\gamma1$-$V_\delta1$) retained the conformational epitope defined by mAb 17D1 that is normally restricted to $V_\gamma5^+$ DETCs. Thus, similar to most B cells and $\alpha\beta$ T cells, the epidermal $\gamma\delta$ cell subset is associated more with an antigen receptor conformation than with simple linear epitopes encoded by the particular V_γ and V_δ gene segments normally used by DETCs.

Because other TCRs can create the 17D1$^+$ conformation, it remains to be explained why the DETC repertoire is normally dominated by a single $V_\gamma5$-$V_\delta1$ combination. We propose that the high frequency of the canonical rearrangement of $V_\gamma5$-$J_\gamma1$ and $V_\delta1$-$J_\delta2$ simply reflects the most frequent mechanism used to establish the 17D1 epitope. This high frequency appears to be determined largely by short stretches of nucleotide sequence homology between the V(D)J gene segments (*8*, *18*). Indeed, canonical in-frame $V_\gamma5$-$J_\gamma1$ and $V_\delta1$-$J_\delta2$ rearrangements are common even in mice in which mutations prevent the expression of the TCR (*8*, *25*). Although this can be interpreted as evidence against selection on the DETC TCR, our observation that the 17D1 epitope is commonly conserved among DETCs, even in the absence of the usual TCR $\gamma\delta$ chain pairing, suggests that the functional efficacy of this epitope may have selected for the retention of the short regions of homology, and not vice versa.

Although we have shown that the proportion of 17D1$^+$ cells in $V_\gamma5^{-/-}$ mice is similar to that in $V_\gamma5^{+/+}$ mice, clearly there are 17D1$^-$ DETCs. Likewise, neonatal DETC repertoires of many inbred strains comprise heterogeneous $\gamma\delta$ cells. However, over time, these regularly converge to >95% 17D1$^+$, consistent with 17D1$^+$ cells having a selective functional or developmental advantage in the skin. The basis for this convergence may be resolved by clarification of the ligands for 17D1$^+$ and 17D1$^-$ DETCs. However, it cannot be assumed that the 17D1 epitope on the DETC TCR defines the conformation of the complementarity-determining region (CDR) 3, which, by extrapolation from Ig and TCR$\alpha\beta$, is likely to be an important contact site for antigen. Both an anti-clonotypic antibody and superantigens bind to TCR$\alpha\beta$ conformations mapping partly or wholly outside CDR3 (*26*), and both can markedly and selectively activate the relevant $\alpha\beta$ T cells in vivo. The 17D1 epitope may similarly manifest an equally important conformation of the DETC TCR.

REFERENCES AND NOTES

1. H. C. van der Heyde *et al.*, *J. Immunol.* **154**, 3985 (1995); A. Mukasa *et al.*, *ibid.* **155**, 2047 (1995); S. J. Roberts *et al.*, *Proc. Natl. Acad. Sci. U.S.A.* **93**, 11774 (1996); M. Tsuji *et al.*, *Int. Immunol.* **8**, 359 (1996); R. Sciammas *et al.*, *J. Exp. Med.* **185**, 1969 (1997).
2. W. Pao *et al.*, *Curr. Biol.* **6**, 1317 (1996).
3. M.-H. Delfau *et al.*, *Eur. J. Immunol.* **22**, 2437 (1992).
4. D. M. Asarnow *et al.*, *Cell* **55**, 837 (1988); S. Itohara *et al.*, *Nature* **343**, 754 (1990); A. C. Hayday and W. Pao, *The Encyclopedia of Immunology* (Academic Press, London, in press).
5. R. Tigelaar and J. M. Lewis, *J. Invest. Dermatol.* **105**, 435 (1995).
6. Of 10^8 129-Agouti.Sv embryonic stem cells electroporated with a 4-kb CsCl-purified, linearized $V_\gamma5$ disruption construct, ~10^3 survived gancyclovir and G418 selection. Of 200 such resistant colonies screened by Southern (DNA) blot hybridization, one (clone 21.2) exhibited a $V_\gamma5$ disruption. Hybridization of Eco RI–cleaved tail DNA with a Bgl II probe (Fig. 1) revealed that 3 (27%) of 11 male chimeras generated from clone 21.2 (by blastocyst injection) and backcrossed to C57BL/6 females transmitted the mutation. Agouti $V_\gamma5^{+/-}$ pups bred to homozygosity showed strict Mendelian statistics of 1:2:1. $V_\gamma5^{-/-}$ offspring displayed no obvious skin or hair abnormalities and were clinically indistinguishable from wild-type littermates.
7. Epidermal sheets were prepared, stained, and examined with a Nikon Optiphot fluorescence microscope [P. Bergstresser and D. V. Juarez, *Methods Enzymol.* **108**, 683 (1984)] and either antibodies to CD3 [biotin-2C11 plus Texas Red–streptavidin (TRSA)], antibodies to TCRδ (GL3 plus biotin-conjugated goat antibodies to hamster IgG plus TRSA), antibodies to $V_\gamma5$ (F536 plus biotin-conjugated goat antibodies to hamster IgG plus TRSA), or mAb 17D1 [1:5 dilution of ammonium sulfate fraction from tissue culture supernatant plus fluorescein isothiocyanate (FITC)–conjugated antibodies to rat IgM]. For DETC quantification, cells were counted in 10 fields of 0.042 mm^2 per specimen, with two to six specimens per mouse. Data are expressed as mean (±SEM) number of positive cells per square millimeter, with *n* values indicating the number of mice examined. Isotype-matched control antibodies yielded consistently negative staining.
8. S. Itohara *et al.*, *Cell* **72**, 337 (1993).
9. C. A. Mallick-Wood *et al.*, *Proc. Natl. Acad. Sci. U.S.A.* **93**, 9704 (1996).
10. *Staphylococcus aureus* Cowan I strain (SACI) (Pansorbin cells; Calbiochem) was coated for 1 hour with either normal hamster IgG, mAb 3A10 to TCRδ (provided by S. Tonegawa), or rabbit antibodies to rat IgM followed by either normal rat IgM or 17D1. DETC clone 1D2 cells were surface-labeled with ^{125}I by lactoperoxidase, and lysed in 1% NP-40. Lysates were pretreated for 30 min once with uncoated SACI and twice with SACI coated with control antibody, and then incubated for 1 hour with SACI coated with each of the control or test antibodies; all manipulations were performed at 4°C. After extensive washing, bound proteins were eluted, reduced, and analyzed by SDS–polyacrylamide gel electrophoresis (PAGE) on 11% gels and autoradiography.
11. W. L. Havran *et al.*, *Proc. Natl. Acad. Sci. U.S.A.* **86**, 4185 (1989).
12. J. J. Lafaille *et al.*, *Cell* **59**, 859 (1989).
13. Interface epidermal cells (IECs) were prepared as described [J. L. Nixon-Fulton *et al.*, *J. Immunol.* **141**, 1897 (1988)] and cultured overnight in RPMI 1640 supplemented with 10% fetal bovine serum, 25 mM Hepes, 20 μM L-glutamine, 10 μM sodium pyruvate, 50 μM 2-mercaptoethanol, nonessential amino acids, and penicillin-streptomycin (CRPMI) to allow re-expression of trypsin-sensitive epitopes before fluorescence-activated cell sorting (FACS) analysis. IEC and DETC lines and clones were stained with antibodies to CD3 (biotin-2C11), anti-TCRδ (FITC-GL3), anti-$V_\gamma5$ (FITC-F536), mAb 17D1 (ammonium sulfate fraction plus phycoerythrin-conjugated goat antibodies to rat IgM), anti-$V_\gamma1$ (2.11) (provided by P. Pereira) [P. Pereira *et al.*, *J. Exp. Med.* **182**, 1921 (1995)], anti-$V_\delta4$ (FITC-GL2), anti-$V_\gamma4$ (biotin-UC3), or anti-$V_\gamma7$ (biotin-GL1) (provided by L. Lefrancois). Biotinylated antibodies were visualized with phycoerythrin-streptavidin. Isotype-matched control antibodies were used at the same concentrations as test antibodies. Analysis was performed with a FACScan (Becton Dickinson, Mountain View, CA), with electronic gates set on live cells by a combination of forward and side light scatter and propidium iodide exclusion. A minimum of 10^4 live events was collected per sample and data were analyzed with Cellquest software.
14. Total RNA was extracted from homogenized cells with the use of silica gel–based spin columns (Qiagen) and was incubated with murine leukemia virus reverse transcriptase and oligo(dT)$_{16}$ (Perkin-Elmer Gene Amp RNA/PCR). PCR amplification was performed with Qiagen Taq DNA polymerase and primers for $V_\gamma1$, $V_\gamma4$, $V_\gamma5$, $V_\gamma6$, or $V_\gamma7$ paired with C_γ, or for $V_\delta1$, $V_\delta4$, or $V_\delta6$ paired with C_δ. The primers were identical to those previously described (*22*) [K. D. Heyborne *et al.*, *J. Immunol.* **149**, 2872 (1992)]. PCR conditions for 30 cycles were 92°C for 1 min (first cycle for 3 min), 52°C for 40 s, and 72°C for 1 min (last cycle for 7 min). PCR products were purified (Qiagen) and sequenced [F. Sanger, S. Niklen, A. R. Coulson, *Proc. Natl. Acad. Sci. U.S.A.* **74**, 513 (1977); F. Toneguzzo *et al.*, *Biotechniques* **6**, 460 (1988)] in the W. M. Keck Foundation BioTechnology Resource Lab at Yale University.
15. DETC lines were prepared by stimulation of IECs (*13*) with concanavalin A (2 μg/ml), IL-2 (10 U/ml), and indomethacin (1 μg/ml), and were cultured in CRPMI containing IL-2 (5 U/ml). From these cells, DETC clones were prepared by limiting dilution, in the absence of feeder cells. Additionally, DETC clones were prepared under the same conditions by limiting dilution of CD3$^+$ IECs in the presence of CD3$^-$ IEC feeders.
16. C. A. Mallick-Wood, unpublished data.
17. A. Ezquerra *et al.*, *Eur. J. Immunol.* **22**, 491 (1992).
18. D. H. Raulet *et al.*, *Immunol. Rev.* **120**, 185 (1991).
19. PCR-RFLP analysis was performed on genomic DNA as described (*27*). $V_\gamma1$-$J_\gamma4$, $V_\gamma5$-$J_\gamma1$, $V_\gamma6$-$J_\gamma1$, and $V_\delta1$-$J_\delta2$ primers and restriction enzyme digestion strategies for $V_\gamma1$-$J_\gamma4$ and $V_\gamma5$-$J_\gamma1$ have been described (*2*, *9*, *27*). $V_\gamma6$-$J_\gamma1$ was digested with Ear I, and $V_\delta1$-$J_\delta2$ with Sha BI, yielding fragments of expected sizes of 72 and 66 bp (±3*n* bp, where *n* = 1, 2, 3 . . .), respectively.
20. G. Stingl *et al.*, *Proc. Natl. Acad. Sci. U.S.A.* **84**, 2430 (1987); J. T. McConnell *et al.*, *J. Immunol.* **142**, 2924 (1989).
21. S. Kyes *et al.*, *Proc. Natl. Acad. Sci. U.S.A.* **86**, 5527 (1989).
22. Y. Takagaki *et al.*, *Nature* **339**, 712 (1989).
23. W. L. Havran, Y.-H. Chien, J. P. Allison, *Science* **252**, 1430 (1991).
24. W. L. Havran and J. P. Allison, *Nature* **335**, 443 (1988); S. Carding *et al.*, *Genes Dev.* **4**, 1304 (1989).
25. D. Asarnow, D. Cado, D. H. Raulet, *Nature* **362**, 158 (1993).

26. D. Housset *et al.*, *EMBO J.* **16**, 4205 (1997); S. C. Hong, G. Waterbury, C. A. Janeway Jr., *J. Exp. Med.* **183**, 1437 (1995).
27. C. A. Mallick *et al.*, *Cell* **73**, 513 (1993).
28. DETC lines 2-10-B6 and 5-6 and clone 30B4 were derived as described (*15*). The transformed keratinocyte line PAM2.12 was provided by A. Takashima. DETCs (10^5 per well) were cocultured with irradiated (30 gray) PAM2.12 keratinocytes (10^5 per well) in 96-well flat-bottom plates for 20 hours at 37°C, after which the extent of PAM2.12 monolayer lysis was noted. Supernatants from the cultures were tested for the ability to support the growth of the IL-2–dependent CTLL cell line (provided by K. Bottomly). CTLL cells were cultured at 5000 cells per well in 96-well round-bottom plates in the presence of medium only (CRPMI), murine recombinant IL-2 (0.01 to 40 U/ml) (Genzyme), or test culture supernatants (dilutions ranging from 1:2 to 1:50). After incubation for 24 hours at 37°C, 1 μCi of [^{3}H]thymidine was added to each well and incubation was continued for an additional 24 hours. Cells were then harvested and [^{3}H]thymidine incorporation was determined.
29. K. Ito *et al.*, *Proc. Natl. Acad. Sci. U.S.A.* **86**, 631 (1989).
30. A. Takashima *et al.*, *J. Invest. Dermatol.* **90**, 671 (1988).
31. K. Heyborne *et al.*, *J. Immunol.* **151**, 4523 (1993).
32. Supported by NIH grants GM37759 and AI27855 (A.C.H.) and AI27404 (R.E.T.). We thank our colleagues for discussion; L. McVay for isolation of genomic clones; T. Taylor for FACS analysis; I. Rosewell and S. Donaldson for mouse work; and M. Bonneville, W. Born, K. Bottomly, L. Lefrancois, P. Pereira, E. Shevach, A. Takashima, and S. Tonegawa for provision of reagents. All animal experiments were performed under accredited conditions after prior approval of protocols by the local Animal Care and Use Committee.

15 October 1997; accepted 20 January 1998

Roles for ORC in M Phase and S Phase

Andrew Dillin and Jasper Rine*

The origin recognition complex (ORC), a six-subunit protein, functions as the replication initiator in the yeast *Saccharomyces cerevisiae*. Initiation depends on the assembly of the prereplication complex in late M phase and activation in S phase. One subunit of ORC, Orc5p, was required at G_1/S and in early M phase. Asynchronous cells with a temperature-sensitive *orc5-1* allele arrested in early M phase. In contrast, cells that were first synchronized in M phase, shifted to the restrictive temperature, and then released from the block arrested at the G_1/S boundary. The G_1/S arrest phenotype could not be suppressed by introducing wild-type Orc5p during G_1. Although all *orc2* and *orc5* mutations were recessive in the conventional sense, this dominant phenotype was shared with other *orc5* alleles and an *orc2* allele. The dominant inhibition to cell-cycle progression exhibited by the *orc* mutants was restricted to the nucleus, suggesting that chromosomes with mutant ORC complexes were capable of sending a signal that blocked initiation on chromosomes containing functional origins.

In *Saccharomyces cerevisiae*, replication initiates from specific DNA sequences called autonomous replication sequences (ARSs), many of which have proven to be chromosomal origins of replication. A six-subunit protein complex, the ORC, binds to ARSs in an ATP-dependent manner and is required for initiation (*1–3*). Homologs of ORC subunits have been identified in other eukaryotes including humans, suggesting that the mechanism by which ORC initiates replication is highly conserved (*4*). Additionally, these homologs are essential for in vitro replication of *Xenopus* egg extracts (*5–7*) and for amplification of the chorion gene cluster of *Drosophila* (*8*).

Eukaryotes can initiate replication at a given origin only once per cell cycle, and there are hundreds of origins whose activation is coordinated. Some origins initiate early and others initiate late in S phase. ORC remains bound to origins throughout the cell cycle (*9*), so initiation of replication, at least in *S. cerevisiae*, is not regulated by simply controlling the binding of ORC to origins.

Division of Genetics, University of California at Berkeley, 401 Barker Hall, Berkeley, CA 94720, USA.

*To whom correspondence should be addressed. E-mail: jrine@uclink4.berkeley.edu

Origin initiation is regulated by a two-step mechanism. The first step, referred to historically as origin licensing, occurs in M phase, and the second step, origin activation, occurs in S phase (*10*). Once a licensed origin has been activated during S phase, it is incapable of initiating again until it is licensed in the next M phase. The factors that make up a licensed origin are not diffusible, because otherwise these factors could diffuse from a late origin that had not initiated to a recently initiated early origin, allowing its reinitiation.

ORC has properties consistent with its being the target of factors that control initiation. From S phase to late M phase, the in vivo footprint at an origin is similar to the footprint created in vitro by purified ORC, suggesting that ORC is the only factor bound during this time. During late M phase, when origins are licensed, the footprint is extended, reflecting the assembly of a prereplication complex (pre-RC) (*9*). Genetic and molecular data suggest that the pre-RC contains ORC, Cdc6p, and the MCM family of proteins (*11–13*). Mutation of the MCM genes causes defects in minichromosome propagation (*14*), and MCM homologs in *Xenopus* are components of licensing factor (*6*, *7*, *15*). The *Xenopus* MCM proteins bind chromatin in an ORC-dependent manner, suggesting that ORC interactions with MCM proteins make an origin competent to initiate replication (*6*).

This study revealed that at least one subunit of the ORC complex, Orc5p, was required for at least two steps in the cell cycle, G_1/S and early M phase. The execution point for the G_1/S function occurred before Start, probably in M phase. Moreover, the level of ORC5 function required for entry into M phase was higher than the level of function required for entry into S phase.

Strains with either *orc2-1* or *orc5-1* recessive mutations are compromised for replication initiation, but differ in their arrest point in the cell cycle upon shift to the nonpermissive temperature. Haploid cells with a defective Orc2 protein (Orc2p) arrest with 1C DNA content (*16*). In contrast, *orc5-1* mutant cells arrest with an apparent 2C DNA content, suggesting that these cells are in G_2 or M phase of the cell cycle (*12*) (Fig. 1) or arrested in late S phase, with most of the genome replicated. A late S phase arrest would suggest that the *orc5-1* allele was defective at a small subset of origins of replication, perhaps the late-initiating ones. Arrest after S phase would argue that the function of Orc5p was not confined to S phase. To distinguish between these possibilities, we examined the arrest phenotype of *orc5-1* mutant cells.

We performed pulsed-field gel electrophoresis (PFGE) on the chromosomal DNA of arrested *orc5-1* cells (*17*). Chromosomal DNA of wild-type (WT) cells arrested in S phase by treatment with hydroxyurea does not enter the gel matrix (*18*). In contrast, the fully replicated chromosomal DNA of cells arrested either in G_1 by α-factor or in M phase by nocodazole entered the gel and migrated in a characteristic manner. By this assay, *orc5-1* cells arrested with a 2C DNA content and contained fully replicated chromosomal DNA similar to that of *orc5-1* cells grown at 23°C and to that of WT cells grown at either 23° or 37°C (Fig. 2).

The *RAD9* checkpoint pathway is activated in response to small amounts of unreplicated and damaged DNA. For example,